



Geophysical Research Letters



RESEARCH LETTER

10.1029/2023GL106377

Key Points:

- High-resolution ocean models with more complete physics are in better agreement with in situ ocean data than coarser resolution models
- Accurate bathymetry is essential to capture circulation pathways and warm water intrusions on the Antarctic continental shelf
- High-resolution ocean models may remain too warm on the continental shelf because they over-predict the sea ice cover

Supporting Information:

Supporting Information may be found in the online version of this article.

Correspondence to:

A. Dinh, andy.dinh@uci.edu

Citation:

Dinh, A., Rignot, E., Mazloff, M., & Fenty, I. (2024). Southern Ocean high-resolution (SOhi) modeling along the Antarctic Ice Sheet periphery. *Geophysical Research Letters*, *51*, e2023GL106377. https://doi.org/10.1029/2023GL106377

Received 15 SEP 2023 Accepted 28 DEC 2023

© 2024. The Authors. This is an open access article under the terms of the Creative Commons Attribution License, which permits use, distribution and reproduction in any medium, provided the original work is properly cited.

Southern Ocean High-Resolution (SOhi) Modeling Along the Antarctic Ice Sheet Periphery

Andy Dinh¹, Eric Rignot^{1,2,3}, Matthew Mazloff⁴, and Ian Fenty³

¹Department Earth System Science, University of California Irvine, Irvine, CA, USA, ²Department Civil and Environmental Engineering, University of California Irvine, Irvine, CA, USA, ³Jet Propulsion Laboratory, California Institute of Technology, Pasadena, CA, USA, ⁴Scripps Institution of Oceanography, University of California San Diego, La Jolla, CA, USA

Abstract The Southern Ocean plays a major role in controlling the evolution of Antarctic glaciers and in turn their impact on sea level rise. We present the Southern Ocean high-resolution (SOhi) simulation of the MITgcm ocean model to reproduce ice-ocean interaction at 1/24° around Antarctica, including all ice shelf cavities and oceanic tides. We evaluate the model accuracy on the continental shelf using Marine Mammals Exploring the Oceans Pole to Pole data and compare the results with three other MITgcm ocean models (ECCO4, SOSE, and LLC4320) and the ISMIP6 temperature reconstruction. Below 400 m, all the models exhibit a warm bias on the continental shelf, but the bias is reduced in the high-resolution simulations. We hypothesize some of the bias is due to an overestimation of sea ice cover, which reduces heat loss to the atmosphere. Both high-resolution and accurate bathymetry are required to improve model accuracy around Antarctica.

Plain Language Summary Warm water from the Southern Ocean melts the glaciers and ice shelves around the Antarctic margin, leading to glacier de-stabilization, and sea level rise. We present the Southern Ocean high-resolution (SOhi) model to better represent ocean circulation and ice-ocean interaction around Antarctica. We assess the accuracy of SOhi with in situ data from marine mammals and compare the results with three other ocean model simulations and to a baseline reference. All model results are slightly too warm on the continental shelf, but the higher-resolution models yield colder waters in better agreement with observations. We attribute the warm bias to an overestimation of the sea ice cover in the ocean models. An improved bathymetry also significantly improves model accuracy in Antarctica.

1. Introduction

The Antarctic Ice Sheet has major impacts on global sea level rise and climate (Intergovernmental Panel on Climate Change (IPCC), 2022; Sadai et al., 2020). A primary driver controlling the evolution of Antarctic glaciers is thermal forcing from the Southern Ocean. In some regions, warm and salty subsurface Circumpolar Deep Water (CDW) (Orsi et al., 1995) is transported onto the continental shelf and into the floating ice shelf cavities (Dinniman et al., 2003; Dotto et al., 2019; Wåhlin et al., 2012). Enhanced thermal energy from CDW melts basal ice at the grounding lines, reduces resistance to glacier flow, allowing the glaciers to speed up and raises sea level (Gudmundsson et al., 2019; Pritchard et al., 2012). At present, these changes in glacier dynamics are the primary drivers of the ice mass loss in Antarctica (Rignot et al., 2008; Velicogna et al., 2014). In areas where the glacier bed elevation drops in the inland direction (i.e., retrograde slope), increased basal melting may trigger a positive feedback loop that puts the glaciers at risk of irreversible retreat (Joughin et al., 2014; Rignot et al., 2014; Weertman, 1974).

Despite its importance, the interaction between the Southern Ocean and the Antarctic Ice Sheet is not well represented in models at present (Nowicki & Seroussi, 2018). The lack of comprehensive and sustained ocean observations along the Antarctic margin makes it difficult to understand ocean dynamics and replicate them in ocean models. Previous modeling studies have shown that coarse-resolution Couple Model Intercomparison Project (CMIP) models cannot capture major physical processes taking place on the continental shelf and cannot reproduce the properties of ocean water masses well (Agosta et al., 2015; Heywood et al., 2014; Meijers, 2014; Purich & England, 2021). These processes include resolving the Antarctic Slope Current (Thompson et al., 2018), interactions between Rossby waves and sea floor troughs (St-Laurent et al., 2013), and eddy heat transport (Stewart & Thompson, 2015). In addition, the ocean state is affected by other factors including sea ice formation

(Jacobs et al., 1970), melt water production (Silvano et al., 2018), winds (Dotto et al., 2019), bathymetry (Silvano et al., 2019), oceanic tides (Richter, Gwyther, King, & Galton-Fenzi, 2022), and polynya (Khazendar et al., 2013).

Here, we present the *Southern Ocean high-resolution* (SOhi) model, a high-resolution simulation of the Massachusetts Institute of Technology general circulation model (MITgcm). SOhi was designed to better reproduce ocean thermal forcing around Antarctica with the inclusion of the most recent bathymetry, thermodynamic sea ice, ocean tides, and all ice shelf cavities. We evaluate the accuracy of SOhi and three other available simulations: (a) the 1/48° model from Estimating the Circulation and Climate of the Ocean consortium (LLC4320; Menemenlis et al., 2021); (b) the Southern Ocean State Estimate (SOSE; Mazloff et al., 2010); and (c) the Estimating the Circulation and Climate of the Ocean version 4 release 4 (ECCO4; ECCO Consortium et al., 2021). Unlike SOhi and LLC4320, SOSE and ECCO4 are ocean state estimates that use observations to constrain the model results. We present the results and discuss their impact on the representation of intrusions of warm water of CDW origin. We conclude with a description of model accuracy at representing ice shelf-ocean interactions in Antarctica.

2. Data and Methods

2.1. MITgcm Simulations

We use two widely used, coarse-resolution, reconstructions of ocean state: (a) SOSE and (b) ECCO4. The models were designed to use observational data to reconstruct the ocean state in a physically consistent manner. SOSE uses the ETOPO5 bathymetry (National Geophysical Data Center, 1993) and has a horizontal grid spacing of 1/6° (4.7 km at 75°S), and 42 vertical levels. ECCO4 uses a modified version of the ETOPO2 bathymetry (National Geophysical Data Center, 2006) and has a horizontal grid spacing of 1°(45 km at 75°S), and 50 vertical levels. The spatial resolutions of SOSE and ECCO4 are too coarse to resolve small scale processes on the continental shelf, but because these models are constrained by observations, they may still perform well at the edge of the continental shelf. We limit the analysis to the period spanning from October 2005 to September 2006, which corresponds to the same time period as SOhi. SOSE and ECCO4 do not include oceanic tides or ice shelf cavities.

The LLC4320 is a 1/48° (0.55–0.94 km at 75°S) simulation spun up from the 1/6° ECCO2 reanalysis. LLC4320 runs on a global Latitude-Longitude-Cap (LLC) grid (Forget et al., 2015) with 90 vertical levels. The bathymetry is from Smith and Sandwell (1997). Climate forcing is from the European Centre for Medium-Range Weather Forecasts (ECMWF) 1/6° operational model analysis (European Centre for Medium-Range Weather Forecasts, 2011). LLC4320 includes oceanic tides but no ice shelf cavities. The LLC4320 simulation covers the period from September 2011 to November 2012 with diagnostics archived as hourly snapshots.

SOhi is a 1/24° (1.2 km at 75°S) simulation starting from 85.5°S and telescoping to 1/12° between 40°S and 30°S. SOhi initial condition is taken from SOSE and the Ocean Comprehensive Atlas (OCCA) (Forget, 2010) (blended together between 25°S and 35°S) with a northern boundary at the equator that matches ECCO4 release 4 (Forget et al., 2015) and atmospheric forcing from ERA-5 (Hersbach et al., 2020). SOhi was spun up for 1 year at 1/12° and mapped to a 1/24° grid starting 1 Jan 2005. We ran SOhi for an additional 9 months before starting our analysis from October 2005 to September 2006. The speed variance (i.e., kinetic energy) is stable over this period (not shown). Diagnostics are archived as 6-hr averages. The bathymetry used in SOhi is an improved version of the General Bathymetric Chart of the Oceans (GEBCO) 2020 bathymetry (GEBCO Bathymetric Compilation Group, 2020, 2020) that includes ice shelf cavities adjusted for local artifacts such as open water within ice shelf domains, water columns thinner than 50 m, and sea floor depths less than 15 m. To better resolve the smaller water column inside the ice cavities, SOhi is divided into 225 vertical levels. For comparison, the z-spacing for SOhi (LLC4320, SOSE, ECCO4) is 1.4 m (1.0, 10.0, 10.0 m) at the surface, 25.8 m (47.3, 142.0, 98.3 m) at 1,000 m, and 50 m (157.8, 250.0, 272.5 m) at 3,000 m. SOhi includes oceanic tides and thermodynamically active ice shelves.

2.2. MEOP Data

To evaluate the models, we use in situ measurements of temperature and salinity from the Marine Mammals Exploring Oceans from Pole to Pole (MEOP; Roquet et al., 2013; Treasure et al., 2017) data set. The MEOP data set is derived from conductivity-temperature-depth (CTD) data loggers mounted on marine mammals that provide temperature and salinity during the animals' dives. MEOP observations provide an abundance of data in shallow

DINH ET AL. 2 of 11

waters near ice shelves, thus giving a reasonable circumpolar coverage of ocean conditions on the continental shelf (Charrassin et al., 2008; Narayanan et al., 2019).

We focus on the waters shoreward of the 1,000 m isobath in the GEBCO bathymetry and below 400 m, as these waters are more likely transported into ice cavities to reach grounding lines (400–2,500 m deep) and melt basal ice. Below 400 m depth, the water temperature is comparable between the summer (October–March) and winter months (April–September) (Figure S1 in Supporting Information S1). As a result, we combine all monthly data into a single yearly mean. The error was calculated by mapping the mean model outputs to the location of MEOP observations using nearest neighbor interpolation. The conversion from MEOP in situ temperature to potential temperature requires knowledge of the salinity (which is not available for all MEOP profiles). To maximize the number of observations, we convert the modeled potential temperature into in situ temperature using the Gibbs SeaWater (GSW) Oceanographic Toolbox of TEOS-10 (McDougall & Barker, 2011). To minimize biases caused by the uneven distribution of MEOP observations, mismatch between models and observations are binned into a 0.5° longitude by 0.2° latitude by 20 m in the vertical. We focus on the 9 regions with the most MEOP data along the periphery of Antarctica: (a) Prince Olav Coast (30°–55°E), (b) Pryzd Bay (69°–83°E), (c) Vincennes Bay (105°–112°E), (d) Adelie Coast (130°–140°E), (e) Ross Sea (160°–175°E), (f) Amundsen Sea Embayment (242°–260°E), (g) Bellingshausen Sea (265°–285°E), (h) Antarctic Peninsula (285°–300°E) and (i) Weddell Sea (318°–355°E).

2.3. ISMIP6 Temperature Reconstruction

The ISMIP6 temperature reconstruction was generated to establish a present day baseline and document how temperature anomalies on the continental shelf of Antarctica may propagate into ice shelf cavities (Jourdain et al., 2020). The ISMIP6 product has been used by ice sheet modelers to project the response of the Antarctic Ice Sheet to different Representative Concentration Pathway for CMIP Phase 6 (Seroussi et al., 2020). The baseline reconstruction uses data spanning 23 years using NOAA World Ocean Atlas 2018 (Locarnini et al., 2018; Zweng et al., 2019), Met Office EN4 subsurface ocean profiles (Good et al., 2013), and MEOP data (Roquet et al., 2013). Observations have been binned and averaged into an 8 km horizontal by 60 m vertical grid, interpolated to fill in data gaps, and extrapolated into the ice shelf cavities using BEDMAP2 bathymetry (Fretwell et al., 2013). The horizontal interpolation accounts for topographic features such as barriers and troughs in the seafloor that limit or facilitate the intrusion of warm water, respectively. The ISMIP6 baseline extends into marginal areas currently covered by ice to account for future glacial retreat that will expose newly un-grounded glacier areas to ocean water.

We use the ISMIP6 temperature reconstruction to evaluate the ability of models to replicate temperature anomalies on the sea floor. Anomalies in temperature, rather than the mean, are used to evaluate how SOhi and LLC4320 propagate changes from the edge of the continental shelf to the ice shelf fronts versus ISMIP6. These temperature anomalies are caused by important factors, for example, CDW intrusions along bathymetric troughs. The anomalies help identify areas of enhanced ocean heat transport across the continental shelf to the ice shelf cavities. We exclude SOSE and ECCO4 from this comparison because they do not resolve the continental shelf in portions of East Antarctica and their spatial resolution is too coarse to capture important physical processes relevant for CDW intrusions.

2.4. Sea Ice Concentration

We compare the seasonal sea ice concentration of four models against the daily sea ice index from NSIDC (Fetterer et al., 2017) and the regional ocean model in Nakayama et al. (2018). The sea ice concentration product has an accuracy of ± 0.05 –0.15 (Windnagel, 2023). We evaluate the model outputs using observations from the same temporal period of each respective model run. This corresponds to the 2011–2012 for LLC4320 and 2005–2006 for the remaining models. Sea ice concentration for the Amundsen Sea is calculated using the original model grid over a domain spanning 99 to 135°W and 68 to 75.5°S. We also analyze the error in austral winter sea ice concentration over the entire continent by remapping the sea ice concentration in the four models and the daily sea ice observations into a 5 km by 5 km grid using nearest neighbor interpolation.

DINH ET AL. 3 of 11

19448007, 2024, 3, Downloaded from https://agupubs.onlinelibrary

Wiley Online Library on [03/07/2024]. See the Terms and Conditions (https://onlinelibrary.wiley.com/terms-and-conditions) on Wiley Online Library for rules of use; OA articles are governed by the applicable Creative Commons

3. Results

3.1. Comparison of the Ocean Models With MEOP

We select 9 regions with an abundance of MEOP observations and good spatial and vertical coverage. We quantify the temperature and salinity bias by depth and longitude, including regional values for the mean error below 400 m (Figure 1). We find a warm bias in all four simulations across the majority of the Antarctic continental shelf. In Pryzd bay (region 2), SOhi is similar to SOSE and ECCO4 with a mean warm bias of $1.5 \pm 0.4^{\circ}$ C. LLC4320 is less than half as warm $(0.6 \pm 0.5^{\circ}\text{C})$. Further East, in Vincennes Bay (region 3) and Adelie Coast (region 4), the high-resolution results (SOhi and LLC4320) have temperature biases $(0.4-1.0^{\circ}\text{C})$ 1°C lower than SOSE and ECCO4 $(1.4-1.7^{\circ}\text{C})$. LLC4320 $(0.6 \pm 0.9^{\circ}\text{C})$ is the most accurate in Vincennes Bay. SOhi $(0.4 \pm 0.5^{\circ}\text{C})$ is the most accurate along Adelie coast. In the Amundsen Sea (region 6), the warm bias is 1.3°C in the coarse resolution models versus $0.9-1.1^{\circ}\text{C}$ in the high-resolution models. The bias is low in the Bellingshausen Sea (region 7) (0.4°C) in all models. In the Antarctic Peninsula (region 8), we find a cold bias in SOhi $(-1.2 \pm 0.6^{\circ}\text{C})$ and LLC4320 $(-1.3 \pm 0.6^{\circ}\text{C})$ not present in SOSE $(0.0 \pm 0.3^{\circ}\text{C})$ and ECCO4 $(0.3 \pm 0.3^{\circ}\text{C})$.

The average vertical profiles of temperature and salinity (Figure 2) in the 9 regions document how the biases vary with depth. Except for the Antarctic Peninsula, the higher resolution models have an accuracy level similar to or better than the coarser models. For example, SOhi and LLC4320 have lower bias in Vincennes Bay (Figure 2c) and Adelie Coast (Figure 2d) where SOSE and ECCO4 are too warm and beyond the range of variability of

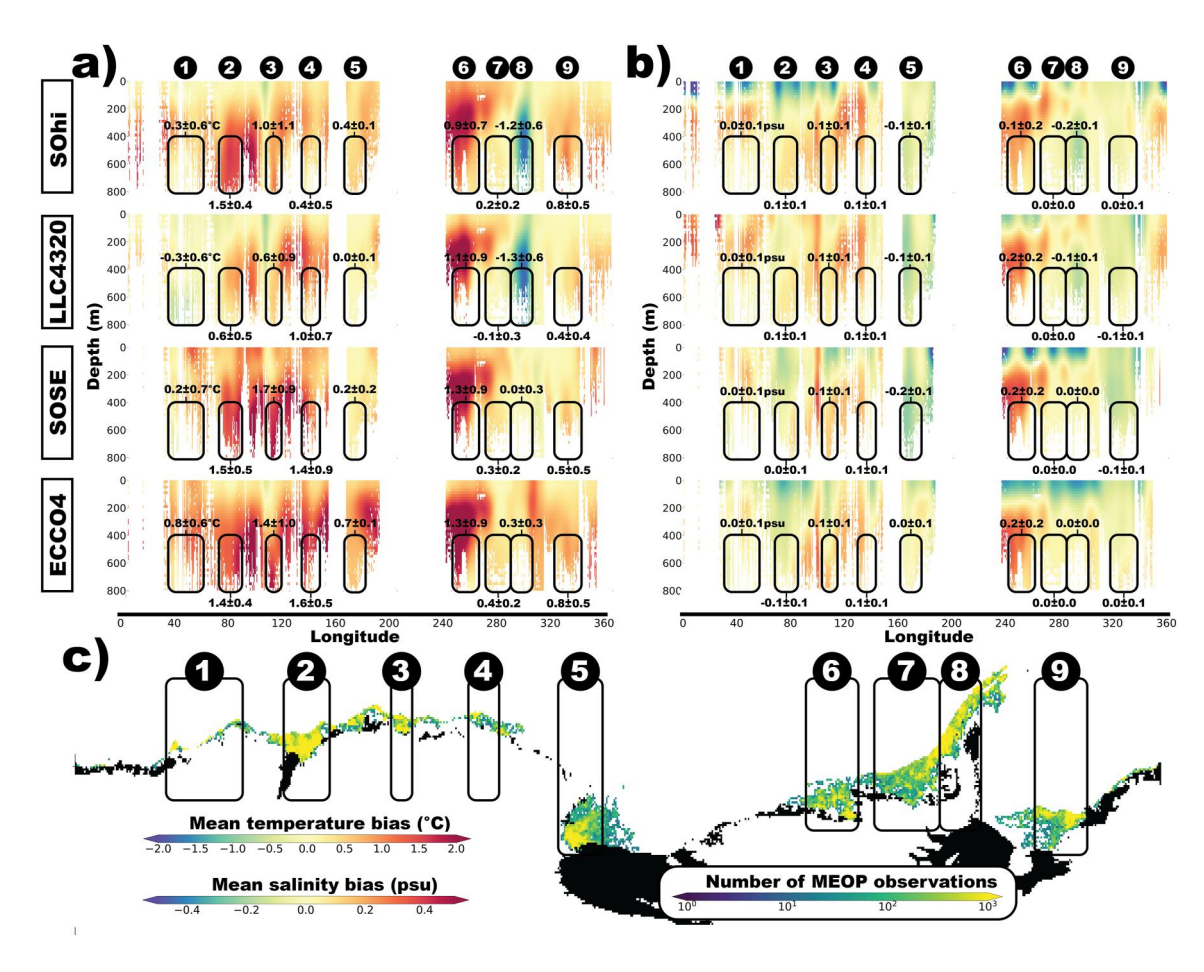


Figure 1. Comparison of temperature and salinity of four MITgcm simulations with MEOP in situ data. Mean model—observation error (averaged across all latitudes on the continental shelf) for (a) temperature (°C) and (b) salinity (psu) of the four MITgcm ocean model simulations (SOhi, LLC4320, SOSE, and ECCO4). Regional mean bias values for the water mass below 400 m are provided. Distribution of MEOP observations and boundary of the nine regions are provided in panel (c). The 9 regions with the most MEOP data are: (1) Prince Olav Coast, 2) Pryzd Bay, 3) Vincennes Bay, 4) Adelie Coast, 5) Western Ross Sea, 6) Amundsen Sea, 7) Bellingshausen Sea, 8) Western Peninsula and 9) Eastern Weddell Sea.

DINH ET AL. 4 of 11

19448007, 2024, 3, Downloaded from https://agupubs.onlinelibrary.wiley.com/doi/10.1029/2023GL106377, Wiley Online Library on [03/07/2024]. See the Terms and Conditions (https://onlinelibrary.wiley.com/terms

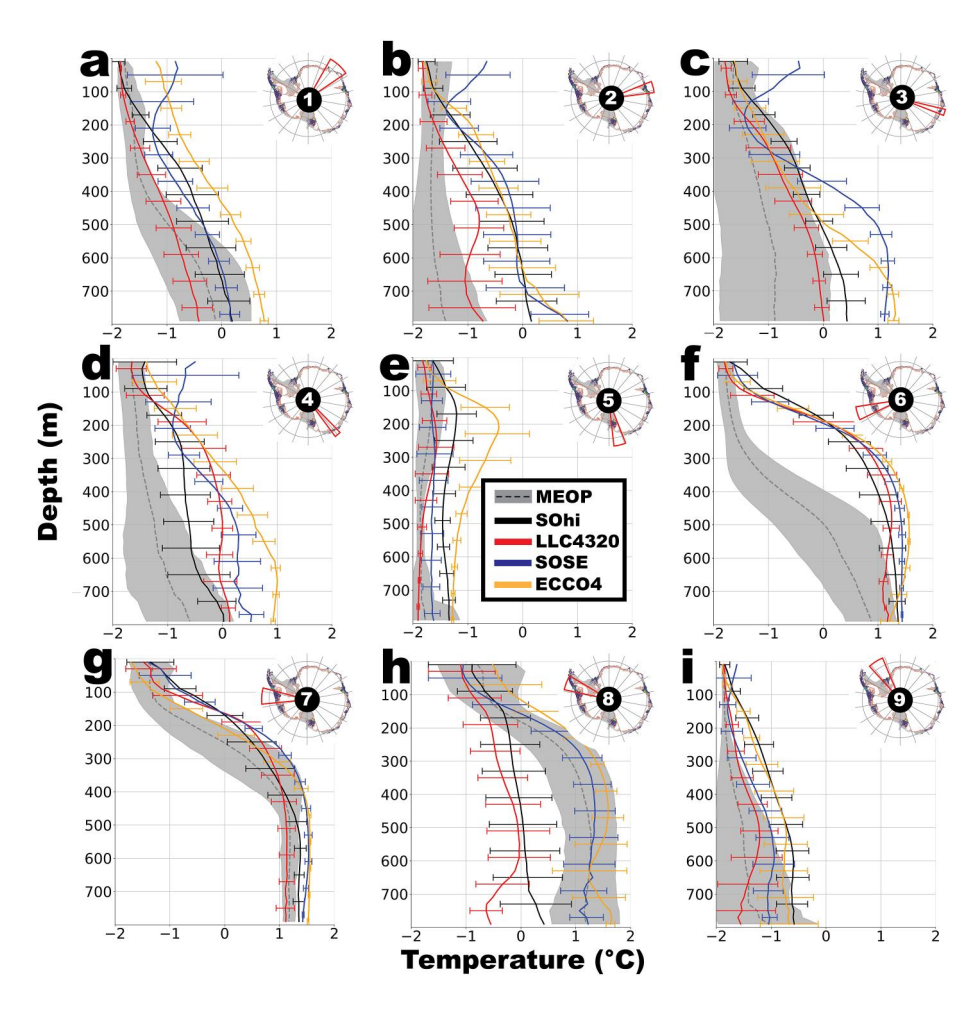


Figure 2. Vertical temperature profiles of four MITgcm simulations versus MEOP in situ data for the 9 regions defined on the inset map of each panel. Shaded regions for MEOP and error bars for the models indicate one standard deviation (1σ) from the mean. Data is binned at 20 m depth increments and smoothed over a 100 m window.

MEOP data (>1°C). In the Amundsen Sea (Figure 2f), the thermocline is 200 m too high in all the models versus observations, but the bias in temperature is negligible at depth and within the range of variability of MEOP.

For salinity, the biases are less than 0.1 psu in East Antarctica and less than 0.2 psu in West Antarctica, Ross Sea, and Weddell Sea (Figure 1; Figure S2 in Supporting Information S1). Vertical profiles of salinity in most regions fall within the range of MEOP observations. Spatially, there is a correlation between the bias in salinity and in temperature, specifically in Wilkes Land (100°–160°) and Amundsen Sea (240°–260°) (Figure 1). Below 400 m, the Pearson correlation coefficients between temperature bias and salinity bias are 0.58–0.68 for East Antarctica (0°–160°E) and 0.78–0.89 for West Antarctica (240°–310°E) (Figure S3 in Supporting Information S1). These numbers suggest that the biases are not in density, but are caused by differences in water mass types.

3.2. Sea Floor Temperature

We compare the anomalies in sea floor temperature in the ISMIP6 reconstruction versus SOhi and LLC4320, excluding SOSE and ECCO4 which are not reliable near ice shelf fronts. We select 4 regions with recent improvements in bathymetry to highlight its impacts on the sea floor temperature anomalies. In the main trough of Fimbul ice shelf (Figure 3a), SOhi and ISMIP6 reproduce a warm anomaly that reaches the grounding line of Jutulstraumen glacier, whereas LLC4320 shows no intrusion due to the missing the seafloor trough leading to the glacier (Nøst, 2004). On Shackleton ice shelf (Figure 3b), SOhi reproduces the intrusion of CDW toward the grounding line of Denman Glacier, which is not included in ISMIP6 or LLC4320. The explanation is the absence of a trough in the sea floor in the (older) bathymetry used by ISMIP6 and LLC4320. On Totten (Figure 3c), the

DINH ET AL. 5 of 11

19448007, 2024, 3, Downloaded from https://agupubs. onlinelibrary.wiley.com/doi/10.1029/2023GL106377, Wiley Online Library on [03/07/2024]. See the Terms and Conditions (https://onlinelibrary.wiley.com/terms-and-conditions) on Wiley Online Library for rules of use; OA articles are governed by the applicable Creative Commons

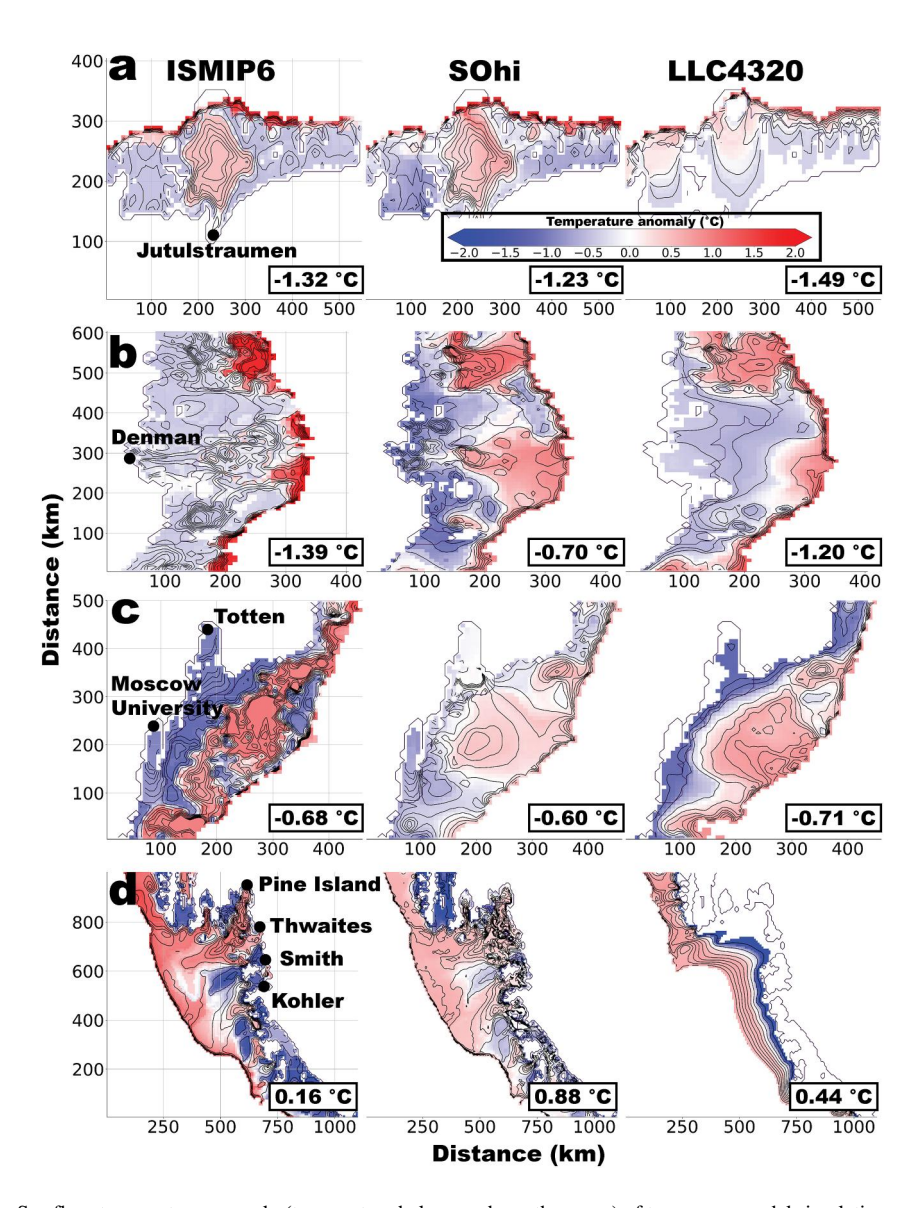


Figure 3. Sea floor temperature anomaly (temperature below or above the mean) of two ocean model simulations versus the ISMIP6 baseline for (a) Fimbul Ice Shelf; (b) Shackleton Ice Shelf; (c) Totten and Moscow University Ice Shelf, and (d) the Amundsen Sea Embayment. The mean temperature that is removed to get the anomaly is provided in the bottom right of each panel. Black contour lines indicate bathymetry at 100 m increments up to a maximum of 1,000 m depth.

two high-resolution models and ISMIP6 reproduce the intrusion of CDW on the continental shelf documented elsewhere (Rintoul et al., 2016), but a colder layer along the coast insulates Totten Glacier in ISMIP6 and LLC4320, whereas CDW reaches the cavity in SOhi thanks to a better bathymetry (Silvano et al., 2019). In the Amundsen Sea (Figure 3d), the LLC4320 model is unable to reproduce the intrusion of CDW because it uses a poor bathymetry with an anomalously steep southerly gradient. SOhi reveals the pathways for CDW, consistent with ISMIP6, which is constrained by numerous observations in that sector.

3.3. Sea Ice Concentration

We compare the seasonal sea ice concentration in the Amundsen Sea (225°–261°E; 75.5°–68°S) (Figure 4a) in SOhi, LLC4320, SOSE, and ECCO4 versus satellite observations of sea ice cover (Fetterer et al., 2017) and outputs from a regional ocean model Nakayama et al. (2018). We find that the large-scale models overestimate the sea ice concentration by 10%–20% in winter. In addition, the melt season in SOhi, LLC4320, SOSE, and ECCO4 is shortened, with sea ice melting later and regrowing sooner than observations. The regional model in Nakayama

DINH ET AL. 6 of 11

1944/807, 2024, 3, Downloaded from https://agupubs.onlinelibrary.wiley.com/doi/10.1029/2023GL106377, Wiley Online Library on [03:07/2024]. See the Terms and Conditions (https://onlinelibrary.wiley.com/terms-and-conditions) on Wiley Online Library for rules of use; OA articles are governed by the applicable Creative Commons Licens

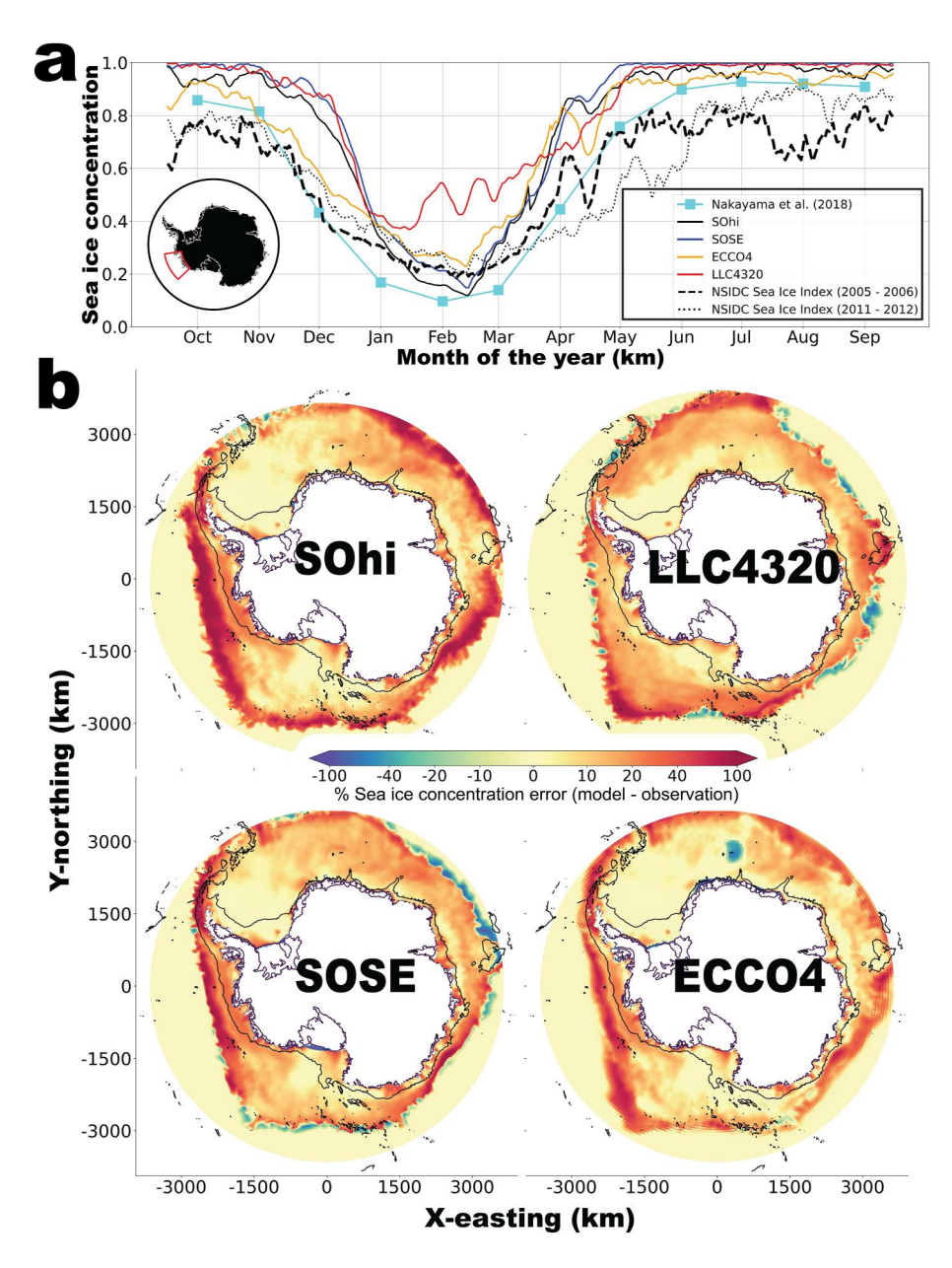


Figure 4. Sea ice concentration of various ocean model simulations versus satellite observations (Fetterer et al., 2017) for SOhi, SOSE, ECCO4, LLC4320 and the regional ocean model in Nakayama et al. (2018) for the Amundsen Sea Embayment sector of West Antarctica (area is Lon: 99–135° West; Lat: 68–75.5° South with coverage shown in inset) and (b) percentage error (model minus observation) in sea ice concentration in August for all of Antarctica for SOhi, LLC4320, SOSE, and ECCO4. Note that the sea ice index used to evaluate LLC4320 is 2011–2012 (rather than 2005–2006) due to the temporal mismatch between LLC4320 and the other models.

et al. (2018) uses different parameters regulating atmosphere-sea ice-ocean heat exchange and exhibits a reduced bias during winter and a more accurate sea ice melt and growth cycle. Sea ice concentration errors between the model outputs and satellite observations for August are similar between the four models (Figure 4b). Overall, the 4 models overestimate the amount of sea ice cover in the Bellingshausen and Amundsen Sea, West Antarctica, and large portions of the continental shelf in East Antarctica.

4. Discussion

In all 4 simulations, we find a warm bias in temperature on most of the continental shelf that varies spatially and with depth. Due to the high computational cost of SOhi and LLC4320, we are only able to evaluate a single year of

DINH ET AL. 7 of 11

simulation against all MEOP observations spanning 2004 to 2019. Combining all the MEOP observations adds uncertainty to our analysis, but it allows us to maximize spatial coverage on the continental shelf. In some regions, such as the Amundsen Sea Embayment, significant interannual variability results in a pycnocline that varies between 400 and 600 m (Dutrieux et al., 2014). In comparison, the pycnocline in the models resides around 200 m, beyond the range of the observed variability. In East Antarctica, the temperature bias near the seafloor is almost 2°C in some regions. As such, in areas with a significant error, we expect that interannual variability will alter the magnitude, but not the direction, of the biases. The warm bias on the continental shelf could impact the modeling of ice-ocean interactions in Antarctica. Ice sheet models, for example, the Ice-sheet and Sea-level System Model (ISSM) (Larour et al., 2012), use the mean temperature and salinity in front of the ice shelf as inputs to the Potsdam Ice-shelf Cavity mOdel (PICO) (Reese et al., 2018) or its variant PICOP (Pelle et al., 2019) to derive basal melt rates. There is strong correlation between the mean cavity temperature and the ice shelf basal melt rates. For example, in SOhi, the correlation between Pine Island ice shelf basal melt rates and mean cavity temperature is 0.989 and the regression coefficient is 3.7 mYr⁻¹ C⁻¹. The presence of a warm bias in the ocean model can possibly result in an overestimation of thermal forcing and basal melt rates in the cavities.

The warm bias is reduced in the higher resolution models which produce colder water on the continental shelf. In a number of prior studies, higher resolution models produced more eddy transport of ocean heat onto the shelf (Dinniman et al., 2016; Nakayama et al., 2014) and hence obtained a warming signal. In contrast, a cooling of Antarctica in the Whole Antarctic Ocean Model (WAOM) was observed when the model resolution increased from 10 to 4 km, with further cooling in East Antarctica at 2 km resolution (Richter, Gwyther, Galton-Fenzi, & Naughten, 2022). The authors attributed the cooling to better resolved tidal processes. Comparing the high-resolution models (SOhi and LLC4320), which both include tides, with the coarser models (SOSE and ECCO4), which do not, we confirm a reduction in temperature in large portions of East Antarctica and the Amundsen Sea as for WAOM. Additionally, SOhi is initialized from SOSE and shares similar atmospheric forcing. The solutions from SOhi and SOSE, however, diverge within a year of being initialized. Many of the warm shelf areas in SOSE are replaced with dense or fresh shelf waters in SOhi (Figure S4 in Supporting Information S1). A closer examination of the solutions indicates that the speed variance of the coastal and slope currents in SOSE is 2 orders of magnitude lower than SOhi and LLC4320, implying that the high-resolution models are better able to resolve physical processes that are missing in SOSE.

In the Amundsen Sea, the warm bias decreases at depth and is within observational uncertainties. The 700-m depth contour coincides with the depth of the limiting sills that protect Pine Island, Thwaites, Smith and Kohler glaciers from CDW intrusions (Millan et al., 2017). Our analysis reveals that the warm signal in this region is not the result of a temperature bias but of a pycnocline that is too shallow (Figure 2f), resulting in too much CDW intrusion to the shelf. Nakayama et al. (2017) lowered the depth of the pycnocline by modifying the coefficients controlling the atmosphere—sea ice—ocean heat fluxes. In our evaluation of sea ice cover versus observations, we find that the model of Nakayama et al. (2018) with adjustments similar to Nakayama et al. (2017) agrees with observations, while all large-scale models overestimate it by 10%-20% in winter and with a shortened melt season. The overestimation of winter sea ice extends across most of Antarctica, especially the Amundsen Sea sector and large swaths of the continental shelf in East Antarctica (Figure 4b). Correcting the sea ice in the largescale models could yield similar bias reduction as Nakayama et al. (2018) by exposing more ocean surface to the atmosphere, increasing turbulence, heat loss, and deepening the pycnocline. However, in some regions, a reduction in sea ice could have the opposite effect due to less brine rejection resulting in less vertical mixing. Nevertheless, sea ice cover has important implications for processes on the continental shelf and should be accurately represented in the models. We conclude that parameter adjustments similar to Nakayama et al. (2018) may be relevant for the larger scale models, for example, SOhi, to more accurately capture sea ice cover on the continental shelf and potentially reduce temperature bias in some sectors.

Previous works noted the importance of model resolution (St-Laurent et al., 2013; Stewart & Thompson, 2015; Stewart et al., 2018) for capturing cross-shelf heat transport processes. Both SOhi and LLC4320 are high-resolution models capable of resolving eddy processes on the continental shelf, yet the accuracy of SOhi is superior to LLC4320 in several key regions, for example, the Amundsen Sea Embayment, Totten, and Fimbul because LLC4320 uses a poor bathymetry in these regions (Figure 3). Accurate bathymetry includes more troughs in front of Totten, Fimbul, and the Amundsen Sea Embayment sector of West Antarctica. The anomalously smooth bathymetry in LLC4320 prevents warm anomalies from reaching any ice shelf in the Amundsen Sea Embayment sector. This example illustrates the essential need to use reliable bathymetry.

DINH ET AL. 8 of 11



Geophysical Research Letters

10.1029/2023GL106377

The improvement in bathymetric mapping is relevant to the ISMIP6 reconstruction. In front of Totten, where the ISMIP6 bathymetry does not include bathymetric troughs, the temperature reconstruction shows no intrusion of CDW. In situ observations from autonomous floats in front of Shackleton Ice Shelf (van Wijk et al., 2022) and Totten (Rintoul et al., 2016), however, indicate the presence of warmer modified CDW in front of these ice shelves, consistent with SOhi. As more areas of the continental shelf are surveyed, for example, as part of SEABED 2030 (Mayer et al., 2018), we expect that the solutions from high-resolution models will become increasingly more accurate at replicating mean temperature, salinity, and anomalies.

In addition to improved bathymetry and better representation of physical processes on the shelf, SOhi includes all ice shelf cavities with thermodymically active ice shelves. Our model analysis quantified how well the model reconstructs the boundary conditions at the entrance of the ice shelf cavities. Future work will focus on the effect of ice shelf melt water on continental shelf processes and on evaluating ice shelf melt rates from SOhi. After 1 year of model run, cavities initialized with SOSE have not fully flushed out the warm water present from the initial condition. A longer simulation is required to enable the assessment of modeled ice shelf melt rates.

5. Conclusions

We evaluate coarse-resolution and high-resolution ocean models of the Southern Ocean with MEOP in situ data and ISMP6 baseline reconstruction. We find a warm bias below 400 m depth on most of the continental shelf in all four models, but the bias is significantly reduced in the higher resolution simulations. In several regions, large differences between high-resolution models are directly attributed to the use of poor bathymetry. In a few areas of high importance for sea level projections, the SOhi model results are more consistent with oceanographic surveys than the ISMIP6 reconstruction because SOhi uses improved bathymetry. Hence, both higher resolution and improved bathymetry are essential to provide a realistic reconstruction of the ocean state on the continental shelf and in front of ice shelves in Antarctica. Finally, we find that the models overestimate the sea ice cover, which could limit air-sea heat exchange. The pan-Antarctic overestimation of sea ice cover may be the root cause for the residual warm bias of the high-resolution models on the continental shelf and deserves future study. From this assessment and given these documented limitations, the SOhi reconstructions already provides one of the most advanced models around Antarctica of relevance to the study of ice-ocean interactions, and in turn of ice sheet evolution.

Data Availability Statement

The MEOP data set was obtained from Roquet et al. (2021). Sea ice index is from Fetterer et al. (2017). ISMIP6 baseline reconstruction can be requested through Ghub at https://theghub.org/dataset-listing. SOSE outputs were obtained from http://sose.ucsd.edu. ECCOv4r4 and LLC4320 is available through NASA NAS server at https://data.nas.nasa.gov/ecco/data.php?dir=/eccodata/llc_90/ECCOv4/Release4 and https://data.nas.nasa.gov/ecco/data.php?dir=/eccodata/llc_4320. SOhi temperature and salinity fields are available on Dryad at Dinh et al. (2024). Codes used to process data and generate the figures are archived at Dinh (2023).

References

Agosta, C., Fettweis, X., & Datta, R. (2015). Evaluation of the CMIP5 models in the aim of regional modelling of the Antarctic surface mass balance. *The Cryosphere*, 9(6), 2311–2321. https://doi.org/10.5194/tc-9-2311-2015

Charrassin, J.-B., Hindell, M., Rintoul, S. R., Roquet, F., Sokolov, S., Biuw, M., et al. (2008). Southern ocean frontal structure and sea-ice formation rates revealed by elephant seals. *Proceedings of the National Academy of Sciences of the United States of America*, 105(33), 11634–11639. https://doi.org/10.1073/pnas.0800790105

 $Dinh,\ A.\ (2023).\ ah-dinh/sh22_si:\ 20231113\ [Software].\ Zenodo.\ https://doi.org/10.5281/zenodo.10121666$

Dinh, A., Rignot, E., Mazloff, M., & Fenty, I. (2024). Monthly mean temperature and salinity outputs from the southern ocean high-resolution (SOhi) simulation [Dataset]. DRYAD. https://doi.org/10.7280/D1V11S

Dinniman, M. S., Asay-Davis, X. S., Galton-Fenzi, B. K., Holland, P. R., Jenkins, A., & Timmermann, R. (2016). Modeling ice shelf/ocean interaction in Antarctica: A review. *Oceanography*, 29(4), 144–153. https://doi.org/10.5670/oceanog.2016.106

Dinniman, M. S., Klinck, J. M., & Smith, W. O. (2003). Cross-shelf exchange in a model of the Ross Sea circulation and biogeochemistry. *Deep-Sea Research Part II: Topical Studies in Oceanography*, 50(22–26), 3103–3120. https://doi.org/10.1016/j.dsr2.2003.07.011

Dotto, T. S., Naveira Garabato, A. C., Bacon, S., Holland, P. R., Kimura, S., Firing, Y. L., et al. (2019). Wind-driven processes controlling oceanic heat delivery to the Amundsen Sea, Antarctica. *Journal of Physical Oceanography*, 49(11), 2829–2849. https://doi.org/10.1175/jpo-d-19-0064.1
Dutrieux, P., Rydt, J. D., Jenkins, A., Holland, P. R., Ha, H. K., Lee, S. H., et al. (2014). Strong sensitivity of pine island ice-shelf melting to climatic variability. *Science*, 343(6167), 174–178. https://doi.org/10.1126/science.1244341

ECCO Consortium, Fukumori, I., Wang, O., Fenty, I., Forget, G., Heimbach, P., & Ponte, R. M. (2021). Synopsis of the ECCO central production global ocean and sea-ice state estimate, version 4 release 4 [Dataset]. Zenodo. https://doi.org/10.5281/zenodo.4533349

Acknowledgments

This work was performed at the University of California Irvine and San Diego and at Caltech's Jet Propulsion Laboratory under Award 80NSSC20K1076 from the National Aeronautics and Space Administration (NASA) Modelling, Analysis, and Prediction (MAP) Program. MRM also acknowledges funding from NASA award 80NSSC22K0387 and NSF awards OCE-1924388, OPP-1936222, and OPP-2319829. We thank Xylar Asay-Davis and one anonymous reviewer for helping to improve the manuscript.

DINH ET AL. 9 of 11

- European Centre for Medium-Range Weather Forecasts. (2011). ECMWF's operational model analysis, starting in 2011 [Dataset]. National Center for Atmospheric Research. https://doi.org/10.5065/D6ZG6O9F
- Fetterer, F., Knowles, K., Meier, W. N., Savoie, M., & Windnagel, A. K. (2017). Sea ice index, version 3 [Dataset]. National Snow and Ice Data Center. https://doi.org/10.7265/N5K072F8
- Forget, G. (2010). Mapping ocean observations in a dynamical framework: A 2004–2006 Ocean Atlas. *Journal of Physical Oceanography*, 40(6), 1201–1221. https://doi.org/10.1175/2009JPO4043.1
- Forget, G., Campin, J.-M., Heimbach, P., Hill, C. N., Ponte, R. M., & Wunsch, C. (2015). ECCO version 4: An integrated framework for non-linear inverse modeling and global ocean state estimation. *Geoscientific Model Development*, 8(10), 3071–3104. https://doi.org/10.5194/gmd-8.3071-2015
- Fretwell, P., Pritchard, H. D., Vaughan, D. G., Bamber, J. L., Barrand, N. E., Bell, R., et al. (2013). Bedmap2: Improved ice bed, surface and thickness datasets for Antarctica. *The Cryosphere*, 7(1), 375–393. https://doi.org/10.5194/tc-7-375-2013
- GEBCO Bathymetric Compilation Group 2020. (2020). The GEBCO_2020 Grid—A continuous terrain model of the global oceans and land. British Oceanographic Data Centre, National Oceanography Centre.
- Good, S. A., Martin, M. J., & Rayner, N. A. (2013). EN4: Quality controlled ocean temperature and salinity profiles and monthly objective analyses with uncertainty estimates: The EN4 data set. *Journal of Geophysical Research: Oceans*, 118(12), 6704–6716. https://doi.org/10. 1002/2013jc009067
- Gudmundsson, G. H., Paolo, F. S., Adusumilli, S., & Fricker, H. A. (2019). Instantaneous Antarctic ice sheet mass loss driven by thinning ice shelves. Geophysical Research Letters. 46(23), 13903–13909. https://doi.org/10.1029/2019g1085027
- Hersbach, H., Bell, B., Berrisford, P., Hirahara, S., Horányi, A., Muñoz-Sabater, J., et al. (2020). The ERA5 global reanalysis. *Quarterly Journal of the Royal Meteorological Society*, 146(730), 1999–2049. https://doi.org/10.1002/qj.3803
- Heywood, K. J., Schmidtko, S., Heuzé, C., Kaiser, J., Jickells, T. D., Queste, B. Y., et al. (2014). Ocean processes at the Antarctic continental slope. *Philosophical Transactions of the Royal Society A*, 372(2019), 20130047. https://doi.org/10.1098/rsta.2013.0047
- Intergovernmental Panel on Climate Change (IPCC). (2022). Sea level rise and implications for low-lying islands, coasts and communities. In *The ocean and cryosphere in a changing climate: Special report of the intergovernmental panel on climate change* (pp. 321–446). Cambridge University Press. https://doi.org/10.1017/9781009157964.006
- Jacobs, S. S., Amos, A. F., & Bruchhausen, P. M. (1970). Ross sea oceanography and Antarctic bottom water formation. Deep-Sea Research and Oceanographic Abstracts, 17(6), 935–962. https://doi.org/10.1016/0011-7471(70)90046-x
- Joughin, I., Smith, B. E., & Medley, B. (2014). Marine ice sheet collapse potentially under way for the Thwaites Glacier Basin, West Antarctica. Science, 344(6185), 735–738. https://doi.org/10.1126/science.1249055
- Jourdain, N. C., Asay-Davis, X., Hattermann, T., Straneo, F., Seroussi, H., Little, C. M., & Nowicki, S. (2020). A protocol for calculating basal melt rates in the ISMIP6 Antarctic ice sheet projections. *The Cryosphere*, 14(9), 3111–3134. https://doi.org/10.5194/tc-14-3111-2020
- Khazendar, A., Schodlok, M. P., Fenty, I., Ligtenberg, S. R. M., Rignot, E., & van den Broeke, M. R. (2013). Observed thinning of Totten glacier is linked to coastal polynya variability. *Nature Communications*, 4(1), 2857. https://doi.org/10.1038/ncomms3857
- Larour, E., Seroussi, H., Morlighem, M., & Rignot, E. (2012). Continental scale, high order, high spatial resolution, ice sheet modeling using the Ice Sheet System Model (ISSM). Journal of Geophysical Research: Earth Surface, 117(F1). https://doi.org/10.1029/2011jf002140
- Locarnini, M., Mishonov, A., Baranova, O., Boyer, T., Zweng, M., Garcia, H., et al. (2018). World Ocean Atlas 2018, volume 1: Temperature (report).
- Mayer, L., Jakobsson, M., Allen, G., Dorschel, B., Falconer, R., Ferrini, V., et al. (2018). The Nippon Foundation—GEBCO SEABED 2030 project: The quest to see the world's oceans completely mapped by 2030. *Geoscience Series*, 8(2), 63. https://doi.org/10.3390/geosciences8020063
- Mazloff, M. R., Heimbach, P., & Wunsch, C. (2010). An eddy-permitting southern ocean state estimate. *Journal of Physical Oceanography*, 40(5), 880–899. https://doi.org/10.1175/2009jpo4236.1
- McDougall, T. J., & Barker, P. M. (2011). In T. J. McDougall (Ed.), Getting started with TEOS-10 and the gibbs seawater (GSW) oceanographic toolbox. Battery point, Tas.
- Meijers, A. J. S. (2014). The Southern Ocean in the Coupled Model Intercomparison Project phase 5. Philosophical Transactions: Mathematical, Physical and Engineering Sciences, 372(2019), 20130296. https://doi.org/10.1098/rsta.2013.0296
- Menemenlis, D., Hill, C., Henze, C. E., Wang, J., & Fenty, I. (2021). Southern ocean pre-SWOT level-4 hourly MITgcm LLC4320 native grid 2km oceanographic dataset version 1.0. NASA Physical Oceanography DAAC. https://doi.org/10.5067/PRESW-ASJ10
- Millan, R., Rignot, E., Bernier, V., Morlighem, M., & Dutrieux, P. (2017). Bathymetry of the Amundsen Sea Embayment sector of West Antarctica from operation IceBridge gravity and other data. Geophysical Research Letters, 44(3), 1360–1368. https://doi.org/10.1002/ 2016s1072071
- Nakayama, Y., Menemenlis, D., Schodlok, M., & Rignot, E. (2017). Amundsen and Bellingshausen Seas simulation with optimized ocean, sea ice, and thermodynamic ice shelf model parameters. *Journal of Geophysical Research: Oceans*, 122(8), 6180–6195. https://doi.org/10.1002/2016jc012538
- Nakayama, Y., Menemenlis, D., Zhang, H., Schodlok, M., & Rignot, E. (2018). Origin of circumpolar deep water intruding onto the Amundsen and Bellingshausen Sea continental shelves. *Nature Communications*, 9(1), 3403. https://doi.org/10.1038/s41467-018-05813-1
- Nakayama, Y., Timmermann, R., Schröder, M., & Hellmer, H. (2014). On the difficulty of modeling Circumpolar Deep Water intrusions onto the Amundsen Sea continental shelf. *Ocean Modelling*, 84, 26–34. https://doi.org/10.1016/j.ocemod.2014.09.007
- Narayanan, A., Gille, S. T., Mazloff, M. R., & Murali, K. (2019). Water mass characteristics of the Antarctic margins and the production and seasonality of dense shelf water. *Journal of Geophysical Research: Oceans*, 124(12), 9277–9294. https://doi.org/10.1029/2018jc014907
- National Geophysical Data Center. (1993). 5-minute gridded global relief data (etopo5). National Geophysical Data Center. https://doi.org/10.
- National Geophysical Data Center. (2006). 2-minute gridded global relief data (etopo2). National Geophysical Data Center. https://doi.org/10.7289/V511012O
- Nøst, O. A. (2004). Measurements of ice thickness and seabed topography under the fimbul ice shelf, dronning Maud land, Antarctica. *Journal of Geophysical Research*, 109(C10), C10010. https://doi.org/10.1029/2004jc002277
- Nowicki, S., & Seroussi, H. (2018). Projections of future sea level contributions from the Greenland and Antarctic Ice Sheets: Challenges beyond dynamical ice sheet modeling. *Oceanography*, 31(2). https://doi.org/10.5670/oceanog.2018.216
- dynamical ice sheet modeling. *Oceanography*, 31(2). https://doi.org/10.56/0/oceanog.2018.216

 Orsi, A. H., Whitworth, T., & Nowlin, W. D. (1995). On the meridional extent and fronts of the Antarctic Circumpolar Current. *Deep Sea Research Part I: Oceanographic Research Papers*, 42(5), 641–673. https://doi.org/10.1016/0967-0637(95)00021-w
- Pelle, T., Morlighem, M., & Bondzio, J. H. (2019). Brief communication: PICOP, a new ocean melt parameterization under ice shelves combining PICO and a plume model. *The Cryosphere*, 13(3), 1043–1049. https://doi.org/10.5194/tc-13-1043-2019

DINH ET AL. 10 of 11

- Pritchard, H. D., Ligtenberg, S. R. M., Fricker, H. A., Vaughan, D. G., van den Broeke, M. R., & Padman, L. (2012). Antarctic ice-sheet loss driven by basal melting of ice shelves. *Nature*, 484(7395), 502–505. https://doi.org/10.1038/nature10968
- Purich, A., & England, M. H. (2021). Historical and future projected warming of Antarctic shelf bottom water in CMIP6 models. Geophysical Research Letters, 48(10), e2021GL092752. https://doi.org/10.1029/2021gl092752
- Reese, R., Albrecht, T., Mengel, M., Asay-Davis, X., & Winkelmann, R. (2018). Antarctic sub-shelf melt rates via PICO. *The Cryosphere*, 12(6), 1969–1985. https://doi.org/10.5194/tc-12-1969-2018
- Richter, O., Gwyther, D. E., Galton-Fenzi, B. K., & Naughten, K. A. (2022). The Whole Antarctic Ocean Model (WAOM v1.0): Development and evaluation. Geoscientific Model Development, 15(2), 617–647. https://doi.org/10.5194/gmd-15-617-2022
- Richter, O., Gwyther, D. E., King, M. A., & Galton-Fenzi, B. K. (2022). The impact of tides on Antarctic ice shelf melting. *The Cryosphere*, 16(4), 1409–1429. https://doi.org/10.5194/tc-16-1409-2022
- Rignot, E., Bamber, J. L., van den Broeke, M. R., Davis, C., Li, Y., van de Berg, W. J., & van Meijgaard, E. (2008). Recent Antarctic ice mass loss from radar interferometry and regional climate modelling. *Nature Geoscience*, 1(2), 106–110. https://doi.org/10.1038/ngeo102
- Rignot, E., Mouginot, J., Morlighem, M., Seroussi, H., & Scheuchl, B. (2014). Widespread, rapid grounding line retreat of Pine Island, Thwaites, Smith, and Kohler glaciers, West Antarctica, from 1992 to 2011. Geophysical Research Letters, 41(10), 3502–3509. https://doi.org/10.1002/ 2014g1060140
- Rintoul, S. R., Silvano, A., Pena-Molino, B., van Wijk, E., Rosenberg, M., Greenbaum, J. S., & Blankenship, D. D. (2016). Ocean heat drives rapid basal melt of the Totten Ice Shelf. Science Advances, 2(12), e1601610. https://doi.org/10.1126/sciadv.1601610
- Roquet, F., Guinet, C., Charrassin, J.-B., Costa, D. P., Kovacs, K. M., Lydersen, C., et al. (2021). Meop-ctd in-situ data collection: A Southern Ocean marine-mammals calibrated sea water temperatures and salinities observations [Dataset]. SEANOE. https://doi.org/10.17882/45461
- Roquet, F., Wunsch, C., Forget, G., Heimbach, P., Guinet, C., Reverdin, G., et al. (2013). Estimates of the Southern Ocean general circulation improved by animal-borne instruments. *Geophysical Research Letters*, 40(23), 6176–6180. https://doi.org/10.1002/2013gl058304
- Sadai, S., Condron, A., DeConto, R., & Pollard, D. (2020). Future climate response to Antarctic Ice Sheet melt caused by anthropogenic warming. Science Advances, 6(39), eaaz1169. https://doi.org/10.1126/sciadv.aaz1169
- Seroussi, H., Nowicki, S., Payne, A. J., Goelzer, H., Lipscomb, W. H., Abe-Ouchi, A., et al. (2020). ISMIP6 Antarctica: A multi-model ensemble of the Antarctic ice sheet evolution over the 21st century. *The Cryosphere*, 14(9), 3033–3070. https://doi.org/10.5194/tc-14-3033-2020
- Silvano, A., Rintoul, S. R., Kusahara, K., Peña-Molino, B., Wijk, E., Gwyther, D. E., & Williams, G. D. (2019). Seasonality of warm water intrusions onto the continental shelf near the Totten Glacier. *Journal of Geophysical Research: Oceans*, 124(6), 4272–4289. https://doi.org/10.1009/2018/sc014634
- Silvano, A., Rintoul, S. R., Peña-Molino, B., Hobbs, W. R., van Wijk, E., Aoki, S., et al. (2018). Freshening by glacial Meltwater Enhances melting of ice shelves and reduces formation of Antarctic bottom water. *Science Advances*, 4(4), eaap9467. https://doi.org/10.1126/sciadv.aap0467
- aap9467
 Smith, W. H. F., & Sandwell, D. T. (1997). Global sea floor topography from satellite altimetry and ship depth soundings. *Science*, 277(5334), 1956–1962. https://doi.org/10.1126/science.277.5334.1956
- Stewart, A. L., Klocker, A., & Menemenlis, D. (2018). Circum-Antarctic shoreward heat transport derived from an eddy- and tide-resolving simulation. Geophysical Research Letters, 45(2), 834–845. https://doi.org/10.1002/2017gl075677
- Stewart, A. L., & Thompson, A. F. (2015). Eddy-mediated transport of warm circumpolar deep water across the Antarctic shelf break. Geophysical Research Letters, 42(2), 432–440. https://doi.org/10.1002/2014g1062281
- St-Laurent, P., Klinck, J. M., & Dinniman, M. S. (2013). On the role of coastal troughs in the circulation of warm circumpolar deep water on Antarctic shelves. *Journal of Physical Oceanography*, 43(1), 51–64. https://doi.org/10.1175/jpo-d-11-0237.1
- Thompson, A., Stewart, A., Spence, P., & Heywood, K. (2018). The Antarctic slope current in a changing climate. *Reviews of Geophysics*, 56(4), 741–770. https://doi.org/10.1029/2018rg000624
- Treasure, A., Roquet, F., Ansorge, I., Bester, M., Boehme, L., Bornemann, H., et al. (2017). Marine mammals exploring the oceans pole to pole: A review of the MEOP consortium. *Oceanography*, 30(2), 132–138. https://doi.org/10.5670/oceanog.2017.234
- van Wijk, E. M., Rintoul, S. R., Wallace, L. O., Ribeiro, N., & Herraiz-Borreguero, L. (2022). Vulnerability of Denman glacier to ocean heat flux revealed by profiling float observations. *Geophysical Research Letters*, 49(18), e2022GL100460. https://doi.org/10.1029/2022g1100460
- Velicogna, I., Sutterley, T. C., & van den Broeke, M. R. (2014). Regional acceleration in ice mass loss from Greenland and Antarctica using
- GRACE time-variable gravity data. Geophysical Research Letters, 41(22), 8130–8137. https://doi.org/10.1002/2014gl061052
 Wåhlin, A. K., Muench, R. D., Arneborg, L., Björk, G., Ha, H. K., Lee, S. H., & Alsén, H. (2012). Some implications of Ekman layer dynamics for
- cross-shelf exchange in the Amundsen Sea. *Journal of Physical Oceanography*, 42(9), 1461–1474. https://doi.org/10.1175/jpo-d-11-041.1 Weertman, J. (1974). Stability of the Junction of an ice sheet and an ice shelf. *Journal of Glaciology*, 13(67), 3–11. https://doi.org/10.1017/s0022143000023327
- Windnagel, A. (2023). Sea ice index, version 3.0. National Snow and Ice Data Center. Retrieved from https://nsidc.org/sites/default/files/g02135-v003-userguide 1 1.pdf
- Zweng, M. R., Jr., Seidov, D., Boyer, T., Locarnini, M., Garcia, H., et al. (2019). World ocean atlas 2018, volume 2: Salinity (report). Retrieved from https://archimer.ifremer.fr/doc/00651/76339/

DINH ET AL.